applied sciences

Supplementary Material: Polarization-Discriminated RSOA-EAM for Colorless Transmitter in WDM-PON

Chengliang Zuo [1] and Xun Li [2,*]

[1] Wuhan National Laboratory for Optoelectronics, Huazhong University of Science and Technology, Wuhan 430074, China; chengliangzuo@gmail.com
[2] Department of Electrical and Computer Engineering, McMaster University, Hamilton, ON L8S 4K2, Canada
* Correspondence: lixun@mcmaster.ca; Tel.: +1-905-525-9140 (ext. 27698)

1. Theoretical Models for the proposed PD RSOA-EAM

1.1 The optical model

The well-established traveling wave model [1,2] incorporating the signal and the broad-band spontaneous emission noise, and the non-uniform carrier and photon distributions along the waveguide is adopted to simulate the device's performance. The entire ASE spectrum is sliced into N_d segments as described in [2]. The slowly varying forward and backward envelopes ($e^f_{TE,TM}$ and $e^b_{TE,TM}$) of the signal and the sliced noise channels are governed by equations as follows:

$$\left(\frac{1}{v_g}\frac{\partial}{\partial t}+\frac{\partial}{\partial z}\right)e^f_{TE,TM}(z,t,\lambda_k) = \left[-\mathrm{j}\left(\frac{1}{2}\alpha_H g_{TE,TM}(z,t,\lambda_k)\right)+\frac{1}{2}\left(\Gamma g_{TE,TM}(z,t,\lambda_k)-\alpha(z)\right)\right]e^f_{TE,TM}(z,t,\lambda_k)+\tilde{s}^f_{TE,TM}(z,t,\lambda_k) \tag{S1a}$$

$$\left(\frac{1}{v_g}\frac{\partial}{\partial t}-\frac{\partial}{\partial z}\right)e^b_{TE,TM}(z,t,\lambda_k) = \left[-\mathrm{j}\left(\frac{1}{2}\alpha_H g_{TE,TM}(z,t,\lambda_k)\right)+\frac{1}{2}\left(\Gamma g_{TE,TM}(z,t,\lambda_k)-\alpha(z)\right)\right]e^b_{TE,TM}(z,t,\lambda_k)+\tilde{s}^b_{TE,TM}(z,t,\lambda_k) \tag{S1b}$$

where the subscripts TE and TM denote the TE and TM polarized electric fields, respectively. λ_k (nm) is the wavelength of the kth (k =1,2, …, N_d) channel in the sliced spectrum, α_H is the linewidth enhancement factor, v_g (m/s) is the group velocity, Γ is the confinement factor, and α (cm^{-1}) is the modal loss. $g_{TE,TM}$ (cm^{-1}) is the material gain of the TE/TM mode that depends on the position in the cavity, the wavelength, and the time. $\tilde{s}^f_{TE,TM}$ and $\tilde{s}^b_{TE,TM}$ (V/m) are the forward and backward spontaneous emission noise, respectively. The noise power contribution in a small section d_z along the propagation direction can be phenomenologically evaluated as [2]:

$$\frac{n_{eff}}{2}\sqrt{\frac{\varepsilon_0}{\mu_0}}\left|\tilde{s}^{f,b}_{TE,TM}(z,t)\right|^2 d_z{}^2=\gamma R^{sp}_{TE,TM}(z,t,\lambda_k)h\nu_k(wd)d_z\,, \tag{S2}$$

where n_{eff} is the effective refractive index, ε_0 (F/m) and μ_0 (H/m) are the permittivity and permeability in a vacuum, respectively. γ is the coupling ratio of the spontaneous emission noise into the waveguide, $R^{sp}_{TE,TM}$ (cm^{-3}s^{-1}) is the spontaneous emission rate, $h\nu_k$ (J) is the photon energy of the kth wavelength channel, and wd (μm^2) is the active region cross-sectional area.

As a Langevin noise source, the amplitude and phase of $\tilde{s}^{f,b}_{TE,TM}(z,t,\lambda_k)$ given in equation (S1) and (S2) can be approximately modeled by the Gaussian and uniformly distributed random processes, respectively. It's therefore expressed as:

$$\tilde{s}^{f,b}_{TE,TM}(z,t)=\left(x_1 e^{ix_2}\right)\left|\tilde{s}^{f,b}_{TE,TM}(z,t)\right|, \tag{S3}$$

where x_1 follows the Gaussian distribution with zero mean and a self-covariance of one, and x_2 follows the uniformly random distribution over [0, 2π].

1.2 The material gain/absorption model

The material gain dispersiveness in the compressively strained quantum well active region of the SOA can be well approximated by [3-5]:

$$g_{TE}(z,t,\lambda_k)=\frac{g_0 \ln\left(N(z,t)/N_0\right)}{1+\varepsilon_S\left[\sum_{k=1}^{N_d}\sum_{i=TE,TM}\left(S_i^f(z,t,\lambda_k)+S_i^b(z,t,\lambda_k)\right)\right]}\left[1-2\left(\frac{\lambda_k-\lambda_c}{\lambda_W}\right)^2\right] \tag{S4}$$

with g_0 (cm^{-1}) denoting the gain coefficient, N_0 (cm^{-3}) the transparent carrier density, ε_S (cm^3) the nonlinear gain suppression coefficient, λ_c (nm) the gain peak wavelength, and λ_W (nm) the full width at half maximum. $S^f_{TE}(z,t,\lambda_k)$, $S^b_{TE}(z,t,\lambda_k)$, $S^f_{TM}(z,t,\lambda_k)$, and $S^b_{TM}(z,t,\lambda_k)$ (cm^{-3}) are the photon densities of the forward TE, backward TE, forward TM, and backward TM optical fields of the *k*th wavelength channel, respectively. The TM material gain $g_{TM}(z,t,\lambda_k)$ is assumed to be zero in the compressively strained quantum well.

The photon density distribution is calculated by:

$$S^{f,b}_{TE,TM}(z,t,\lambda_k)=\frac{n_{eff}}{2h\nu_k}\sqrt{\frac{\varepsilon_0}{\mu_0}}\frac{\Gamma}{wdv_g}\left|e^{f,b}_{TE,TM}(z,t,\lambda_k)\right|^2 \tag{S5}$$

The spontaneous emission rate $R^{sp}_{TE,TM}$ in equation (S2) is related with the material gain through [2,3]:

$$R^{sp}_{TE,TM}(z,t,\lambda_k)=\left(\frac{8\pi n_{eff}^2\nu_k^2\Delta\nu}{c^2}\right)n_{sp}g_{TE,TM}(z,t,\lambda_k) \tag{S6}$$

where $\Delta\nu$ (Hz) is the frequency difference between the adjacent wavelength channels, c (m/s) is the velocity of the light in a vacuum, and n_{sp} is the inversion factor relating the spontaneous emission gain and the material gain [3].

The absorption in the EAM is assumed to be polarization and wavelength independent. A phenomenological model [6] is used to calculate the EAM material absorption:

$$g_{TE,TM}(z,t)=\alpha^{EAM}_{TE,TM}(z,t)=\frac{-a_V\left(V(z,t)-V_{on}\right)^2}{1+P(z,t)/P_{sat}} \tag{S7}$$

where a_V (cm^{-1}V^{-2}) is the absorption constant, *V* (V) is the driving voltage, V_{on} (V) is a reference voltage, and P_{sat} (mW) is the saturation power of the EAM.

1.3 The carrier rate equation

The spatial and time dependent carrier density *N*(*z*,*t*) in the SOA can be solved by the following rate equation:

$$\begin{aligned}\frac{\partial N(z,t)}{\partial t}&=\frac{\eta_i I(z,t)}{eLwd}-\left[AN(z,t)+BN(z,t)^2+CN(z,t)^3\right]\\&-v_g\sum_{k=1}^{N_d}\left\{g_{TE}(z,t,\lambda_k)\left[S^f_{TE}(z,t,\lambda_k)+S^b_{TE}(z,t,\lambda_k)\right]+g_{TM}(z,t,\lambda_k)\left[S^f_{TM}(z,t,\lambda_k)+S^b_{TM}(z,t,\lambda_k)\right]\right\}\end{aligned} \tag{S8}$$

where η_i is the current injection efficiency, *I* (mA) is the injection current, *e* (C) is the electron charge, *L* (μm) is the length of the active region, *A* (s^{-1}), *B* (cm^{-3}s^{-1}), and *C* (cm^{-6}s^{-1}) are the linear recombination coefficient, the bimolecular recombination coefficient, and the Auger recombination coefficient, respectively.

1.4 The boundary conditions

The transmission in the FR is a passive process which induces absorption and phase delay. Since the downstream signal is assumed to be TE (0°) polarized, after its rotation in the FR with an angle of θ_{FR}, the upstream signal TE (e^b_{TE}) and TM (e^b_{TM}) optical fields at the EAM input become:

$$e^b_{TE}(L_{SOA}+L_{EAM},t,\lambda_k)=e^f_{TE}(L_{SOA}+L_{EAM},t,\lambda_k)\sqrt{T_F R_2}\cos(\theta_{FR})\mathrm{e}^{i\Phi} \tag{S9a}$$

$$e^b_{TM}(L_{SOA}+L_{EAM},t,\lambda_k)=e^f_{TE}(L_{SOA}+L_{EAM},t,\lambda_k)\sqrt{T_F R_2}\sin(\theta_{FR})\mathrm{e}^{i\Phi} \tag{S9b}$$

where T_F and Φ denote the round-trip transmission coefficient and the phase delay in the FR, respectively. R_2 is the rear facet power reflectivity.

The powers coupled to and from the proposed device subject to the input/output port boundary conditions:

$$e^f_{TE}(0,t,\lambda_k)=\sqrt{R_1}e^b_{TE}(0,t,\lambda_k)+\sqrt{\frac{2}{n_{eff}}\sqrt{\frac{\mu_0}{\varepsilon_0}}\alpha_{in}(1-R_1)P_{in}(t,\lambda_k)} \tag{S10}$$

$$P^{out}_{TE,TM}(t,\lambda_k)=\frac{n_{eff}}{2}\sqrt{\frac{\varepsilon_0}{\mu_0}}\alpha_{out}(1-R_1)\left|e^b_{TE,TM}(0,t,\lambda_k)\right|^2 \tag{S11}$$

where $P_{in}(t,\lambda_k)$ is the input power, α_{in} is the input coupling loss, α_{out} is the output coupling loss, R_1 is the front facet power reflectivity. $P^{out}_{TE}(t,\lambda_k)$ and $P^{out}_{TM}(t,\lambda_k)$ are the upstream TE and TM mode powers after coupling to the fiber. The total upstream output power is a summation of $P^{out}_{TE}(t,\lambda_k)$ and $P^{out}_{TM}(t,\lambda_k)$.

In summary, equations (S1), (S4), (S7) and (S8), subject to the boundary conditions (S9)-(S11), are solved for the evolution of the carrier and photon density distributions inside the PD RSOA-EAM cavity by the numerical scheme as described in section 2.

2. Numerical Implementation

Since the theoretical models in section 1 generally do not have an analytically solution, a numerical algorithm is therefore required. As shown in Figure S1, the entire device is divided into two sections: the active region including the SOA and the EAM, and the passive region including the FR. The active region is divided into *N* segments along the light propagation direction with equal length d_z, and the passive region is attached to segment *N* of the active region. After the light enters the passive region, it will be reflected back to the active region, accompanied by the polarization rotation, the power loss, and the phase delay. This effect introduced in the passive region can be incorporated into the traveling wave equations by applying the transmission coefficient T_F and phase delay Φ [7] as boundary conditions on the section *N* of the active region, as indicated in equation (S9).

The numerical algorithm generally starts from $N(z,t{=}0)=N_0$ (in the SOA) and $V(z,t{=}0)=V_{on}$ (in the EAM). The initial signal and noise optical fields are set to zero. The material gain $g_{TE}(z,t=0,\lambda_k)$ in the SOA and the material loss in the EAM $\alpha^{EAM}_{TE,TM}(z,t{=}0)$ are calculated from (S4) and (S7), respectively. The optical fields at time $t+\Delta t$ are then obtained from the analytical solution of (S1) after the propagation of length d_z [2]:

$$\begin{aligned} e^f_{TE,TM}(z+\Delta z,t+\Delta t,\lambda_k)=&\left\{\mathrm{e}^{\left(-\frac{j}{2}\alpha_H g_{TE,TM}(z,t,\lambda_k)\right)d_z}\times\mathrm{e}^{\left[\frac{1}{2}\left(\Gamma g_{TE,TM}(z,t,\lambda_k)-\alpha(z)\right)\right]d_z}\right\}e^f_{TE,TM}(z,t,\lambda_k)\\ &+d_z\sqrt{\frac{2}{n_{eff}}\sqrt{\frac{\mu_0}{\varepsilon_0}}\frac{\gamma h\nu_k(wd)}{d_z}R^{sp}_{TE,TM}(z,t,\lambda_k)\cdot r_{ng}} \end{aligned}, \tag{S12a}$$

$$e^r_{TE,TM}(z-\Delta z, t+\Delta t, \lambda_k) = \left\{ e^{\left(-\frac{j}{2}\alpha_H g_{TE,TM}(z,t,\lambda_k)\right)d_z} \times e^{\left[\frac{1}{2}\left(\Gamma g_{TE,TM}(z,t,\lambda_k)-\alpha(z)\right)\right]d_z} \right\} e^r_{TE,TM}(z,t,\lambda_k) + d_z\sqrt{\frac{2}{n_{eff}}\sqrt{\frac{\mu_0}{\varepsilon_0}}\frac{\gamma h\nu_k(wd)}{d_z}R^{sp}_{TE,TM}(z,t,\lambda_k)}\cdot r_{ng} , \qquad \text{(S12b)}$$

where the last term on the right hand side represents the contribution from the spontaneous noise in step d_z, and r_{ng} is a random complex number taken from the random noise generator $x_1 e^{ix_2}$ in (S3). When the optical fields hit the boundary, equations (S9) and (S10) are applied. After obtaining the new set of optical fields, a small current step δI is added onto the SOA and the current at time $t+\Delta t$ becomes: $I(z,t+\Delta t) = (eLwd/\eta_i)\left(AN(z,t)+BN^2(z,t)+CN^3(z,t)\right)+\delta I$. The carrier density $N(z,t+\Delta t)$ is then calculated from the carrier rate equation (S8) by the lower order Runge–Kutta or explicit Euler method. The material gain $g_{TE,TM}(z,t+\Delta t,\lambda_k)$ in the SOA and the material loss in the EAM $\alpha^{EAM}_{TE,TM}(z,t+\Delta t)$ are again calculated from (S4) and (S7) with $N(z,t+\Delta t)$ and $V(z,t+\Delta t)$, respectively. Next update the optical fields $e^{f,r}_{TE,TM}(z,t+2\Delta t,\lambda_k)$ through equation (S12), and then $N(z,t+2\Delta t)$, $g_{TE,TM}(z,t+2\Delta t,\lambda_k)$, and $\alpha^{EAM}_{TE,TM}(z,t+2\Delta t)$ as aforementioned, then all the variables at time $t+3\Delta t$, $t+4\Delta t$, … . The iteration continues until a traversal of the SOA injection current change and the EAM voltage change is completed.

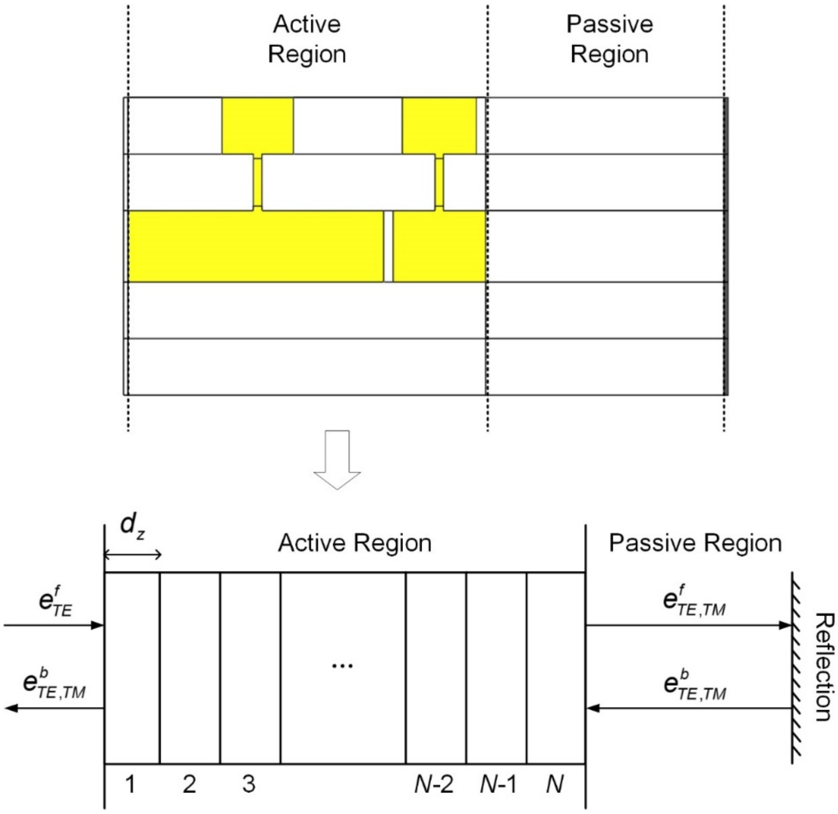

Figure S1. Schematic diagram of the simulation setup for the polarization-discriminated RSOA-EAM.

For the case of static state analysis, the time derivatives in the governing equations should become zero finally. After the current/voltage reached the maximum value, the iteration will stop if no further changes can be detected on the optical fields and the carrier densities.

In summary, the step for steady state and dynamic analysis can be concluded as follow [4]:

a) The steady state analysis procedure

(1) Parameters input.
(2) Longitudinal subdivision (in z direction).
(3) Variables initialization.
(4) Operating condition input (possible looping starts here).
(5) Variable scaling (physical to numerical).
(6) 1D- iteration loop starts.
(7) Solve the carrier rate equation.
(8) Solve the material gain equation.
(9) Solve the traveling wave equation.
(10) Go to the iteration starting point (step 6) if not converged, otherwise continue.
(11) Variable scaling (numerical to physical).
(12) Post processing for required output assembly.
(13) Go to step 4 for operating condition (bias, voltage, input power, or wavelength) looping, until the maximum settings are reached, otherwise continue.
(14) Stop.

b) The dynamic analysis procedure

(1) Parameters input.
(2) Longitudinal subdivision (in z direction).
(3) Variables initialization.
(4) Variable scaling (physical to numerical).
(5) Time domain progression starts.
(6) Operating condition input (read in bias/voltage/input power as function of time).
(7) Solve the carrier rate equation.
(8) Solve the gain equation.
(9) Solve the traveling wave equation.
(10) Go to the progression starting point (step 5) if the maximum time is not reached, otherwise continue.
(11) Variable scaling (numerical to physical).
(12) Post processing for required output assembly.
(13) Stop.

3. Numerical simulation results

3.1. Performance of the single-SOA section and the single-EAM section

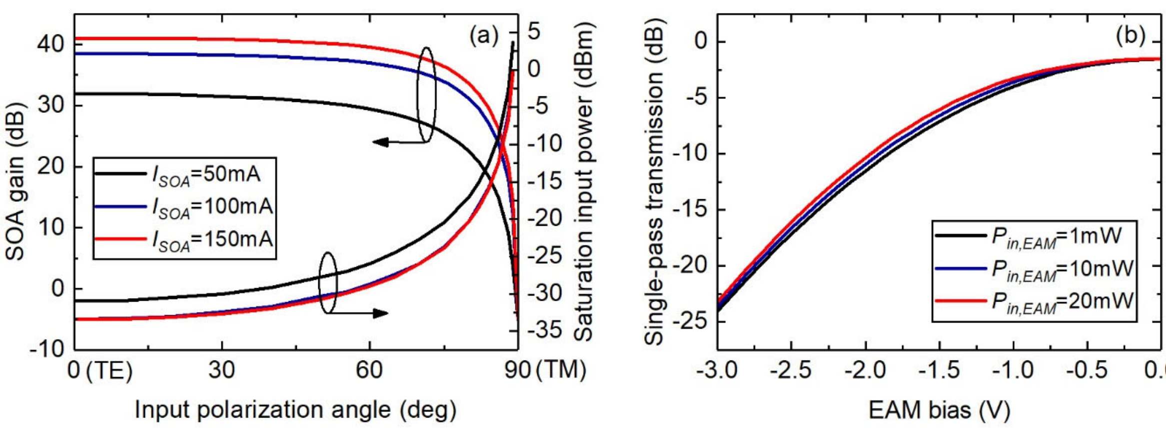

Figure S2. (**a**) Static gain of the single SOA section (at an input power of -25 dBm) and the SOA saturation input power as a function of the input polarization angle. (**b**) Static single-pass extinction curve of the EAM section with different powers injected into the EAM section. ($P_{in,EAM}$: power injected into the EAM section).

3.2. Wavelength dependence of the downstream signal erasing

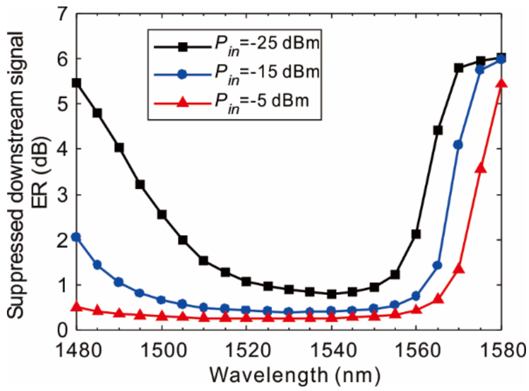

Figure S3. ER of the suppressed downstream signal as functions of the downstream signal wavelength. The rotation angle is 90°.

3.3. Wavelength dependence of the upstream signal at output

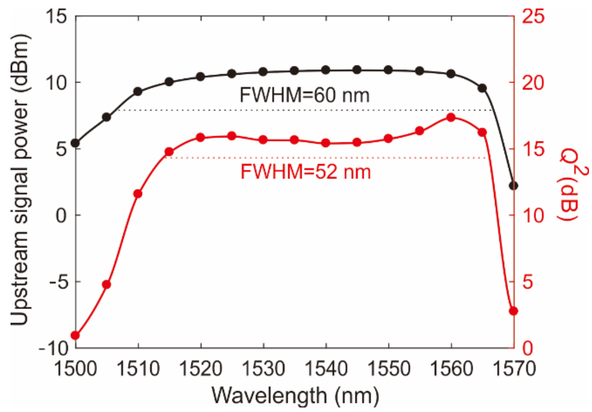

Figure S4. Output power and Q-factor of the upstream signal as functions of the downstream signal wavelength.

References

1. Park, J.; Li, X.; Huang, W.-P. Performance simulation and design optimization of gain-clamped semiconductor optical amplifiers based on distributed Bragg reflectors. *IEEE J. Quantum Electron.* **2003**, *39*, 1415-1423.
2. Park, J.; Li, X.; Huang, W.-P. Comparative study of mixed frequency-time-domain models of semiconductor laser optical amplifiers. *IEE Proceedings-Optoelectronics* **2005**, *152*, 151-159.
3. Agrawal, G.P. *Fiber-optic communication systems*; John Wiley & Sons: 2012; Vol. 222.
4. Li, X. *Optoelectronic devices: Design, modeling, and simulation*; 2009; 10.1017/CBO9780511581144pp. 1-361.
5. Makino, T. Analytical formulas for the optical gain of quantum wells. *IEEE J. Quantum Electron.* **1996**, *32*, 493-501, doi:10.1109/3.485401.
6. Mørk, J.; Kjær, R.; der Poel, M.v.; Yvind, K. Slow light in a semiconductor waveguide at gigahertz frequencies. *Opt. Express* **2005**, *13*, 8136-8145, doi:10.1364/OPEX.13.008136.
7. Zaman, T.R.; Guo, X.; Ram, R.J. Faraday rotation in an InP waveguide. *Appl. Phys. Lett.* **2007**, *90*, 023514, doi:10.1063/1.2430931.